J Mater Sci (2008) 43:5861–5866
DOI 10.1007/s10853-008-2827-3

Preparation of gold/polyaniline/multiwall carbon nanotube nanocomposites and application in ammonia gas detection

Qifei Chang · Kai Zhao · Xing Chen · Minqiang Li · Jinhuai Liu

Received: 12 April 2008 / Accepted: 24 June 2008 / Published online: 28 July 2008
© Springer Science+Business Media, LLC 2008

Abstract Composites of multiwall carbon nanotubes (MWNTs), polyaniline (PANI), and gold nanoparticles were prepared by one pot synthesis. Based on the interaction between aniline monomers and MWNTs, aniline molecules were adsorbed and polymerized on the surface of MWNTs. The nanocomposites were characterized by transmission electron microscopy (TEM), X-ray diffraction analysis (XRD), Fourier transform infrared spectroscopy (FT-IR), and X-ray photoemission spectroscopy (XPS). The sensors based on Au/PANI/MWNT nanocomposites were tested for on-line monitoring of ammonia gas. The results show that the as-prepared sensors have superior sensitivity, and good repeatability upon repeated exposure to ammonia gas.

Introduction

Since discovered by Iijima [1], carbon nanotubes (CNTs) have been attracted a lot efforts to explore and develop their applications. Recently, CNTs have been considered as prime materials for gas adsorption due to their high surface-to-volume ratio, hollow geometry, and unique electrical properties [2–4], which leads to high sensitivities to charged analytes [5]. Gas sensors based on CNTs have been extensively studied and are being emerged both as high sensitive gas detectors [4, 6–12] and for biosensing application [13].

Recent research interest has been focused on the preparation of nanomaterials/nanocomposites involving the combination of CNTs, conducting polymers and metal nanoparticles by employing various methodologies such as sol–gel process, self-assembly, electrochemical, and chemical methods [14–18]. Polyaniline (PANI) is one of the most important conducting polymers with many advantages such as an inexpensive monomer, a simple polymerization reaction with high yield, and excellent stability [19]. On the top of those qualities, PANI has a distinct doping mechanism. Protonation by acid–base chemistry leads to an internal redox reaction and the conversion from a low conductivity emeraldine base into a highly conducting emeraldine salt. This implies that PANI can be used in highly sensitivity sensors for reaction that involve an acid or base, such as NH_3 and HCl gas [20–22]. Besides, attaching the metal nanoparticles onto the surface of nanotubes or to sidewalls to obtain hybrid nanocomposites is gaining interest, which can enhance the sensitivity of the sensors based on CNTs [23].

Ammonia is one of the important industrial exhaust gases with high toxicity [24, 25]. With the increasing of the human awareness of environmental problems in industrial gases, the requirement of detecting these gases has greatly increased. Unfunctionalized CNTs-based sensors have been demonstrated for the detection of NH_3 and NO_2 under ambient conditions [6, 7]. The main sensing mechanism of the sensors based on CNTs has been suggested as an electron-donating/electron-withdrawing charge transfer between the molecules and the semiconducting CNTs, which affected the conductivity of CNTs [6]. However, the

Q. Chang · K. Zhao · X. Chen · M. Li · J. Liu (✉)
The Key Laboratory of Biomimetic Sensing and Advanced Robot Technology, Institute of Intelligent Machines, Chinese Academy of Science, Hefei, Anhui 230031, People's Republic of China
e-mail: jhliu@iim.ac.cn

Q. Chang
Department of Chemistry, University of Science and Technology of China, Hefei, Anhui 230026, People's Republic of China

less than ideal sensitivity and lack of selectivity limits CNTs in practical applications. Recently, many approaches have been developed to functionalized CNTs, including covalent and noncovalent chemical functionalization, and in studies these have shown improved performance as gas sensors. So it is promising to develop a simple and versatile functionalization technique which enables fabrication of CNT-based sensors with improved sensitivity and selectivity.

In this paper, we have established one pot synthesis of the Au/PANI/multiwall carbon nanotubes (MWNTs) nanocomposites. The MWNTs were refluxed in HNO_3 solution, which produced carboxylic acid groups at the defect sites and thus improved the solubility of the carboxylic groups contained MWNTs in HCl solution. When $HAuCl_4$ as the oxidant was mixed with the aniline monomers in the solution, the reduction of $HAuCl_4$ and the oxidization occur simultaneously, leading to the formation of Au nanoparticles and PANI. Based on the interaction between aniline monomers and MWNTs, the PANI was in situ polymerized and absorbed at the surface of the MWNTs with the Au nanoparticles dispersed in. Here we demonstrate that the Au/PANI/MWNTs nanocomposites can be acted as sensors for the detection of ammonia gas. The sensors show a high sensitivity, good reversibility, and repeatability.

Experimental

Reagents

Aniline (Aldrich) was distilled before using. Multiwall carbon nanotubes, MWNTs (diameter is 20–40 nm) obtained from Shenzhen Nanotechnologies Co. Ltd were rinsed with double-distilled water and dried. Nitric acid, methanol, chloroaurate acid, and hydrochloric acid (Analytical grade, Aldrich) were used as received.

Fabrication of the Au/PANI/MWNT nanocomposites

Fifty milligrams of MWNTs were refluxed in 4 M HNO_3 for 24 h and filtered through a polycarbonate membrane (0.2 μm pore size). The product was washed using double-distilled water and dried in vacuum at 60 °C for 12 h. After that, 5 mg MWNT-COOH was added to the solution of aniline (10 mM) with 1 M HCl and then sonicated for 3 h to obtain a homogeous solution. An aqueous solution of $HAuCl_4$ in 1 M HCl was quickly added to the above solution. The mixture was allowed to react at 0–5 °C (in an ice bath) for 12 h with stirring. The product was washed with double-distilled water several times and dried under vacuum at room temperature.

Characterization

Transmission electron microscopy images were recorded on a Hitachi H-800 transmission electron microscope operated at an accelerating voltage of 200 kV. Fourier transform infrared (FT-IR) spectrum of the nanocomposites was recorded using a NEXUS-870 FT-IR spectrophotomer in the region 400–2000 cm^{-1} using KBr pellets. A Philips X'pert-PRO X-ray diffractometer was employed using a Cu-$K\alpha$ source to obtain XRD spectrum of the nanocomposites. XPS measurement of a film of the sample was carried out on a VG ESCALAB MKII instrument at a pressure greater than 10^{-6} Pa.

Measurement of gas sensing

The gold comb-like electrode covered with nanocomposites has been located in a sealed chamber (1 L) with a gas inlet/outlet for gas exposure experiments. The gas sensing experiments have been performed by measuring the electrical conductance of the sensor upon exposing to different concentration of ammonia gas. The dc electrical conductance of the sensor has been measured in the two-pole format by the volt-amperometric technique using 6487 Picoammeter/Voltage Source (Keithley, USA). Then, the sensor was exposed to the selected concentration of ammonia gas until the sensor's response reached a steady value, followed by purging the sensor with dry air until the sensor recovered initial resistance. After that, the sensor was exposed to another concentration of ammonia gas. This process was repeated many times to evaluate the sensitivity, reversibility, and repeatability of the sensor.

Results and discussion

The Au/PANI/MWNT nanocomposites have successfully prepared by a single step or one pot synthesis. The formation mechanism of the Au/PANI/MWNT nanocomposites is believed to arise from strong interaction between aniline monomer and MWNTs. Figure 1 schematically depicts the formation mechanism of Au/PANI/MWNT nanocomposites. This interaction is believed to be caused by the presence of the π–π^* electron interaction, as well as the hydrogen bond interaction between the carboxyl groups of MWNTs and the amino groups of the aniline monomer [26]. Such strong interaction ensures that the aniline monomers are absorbed on the surface of MWNTs, which serve as the core and the self-assembly template during the formation of the tubular nanocomposites. When the aniline monomers are mixed with the chloroaurate acid, the reduction of $HAuCl_4$ and oxidation of aniline monomers occur simultaneously, leading to the formation of gold nanoparticles

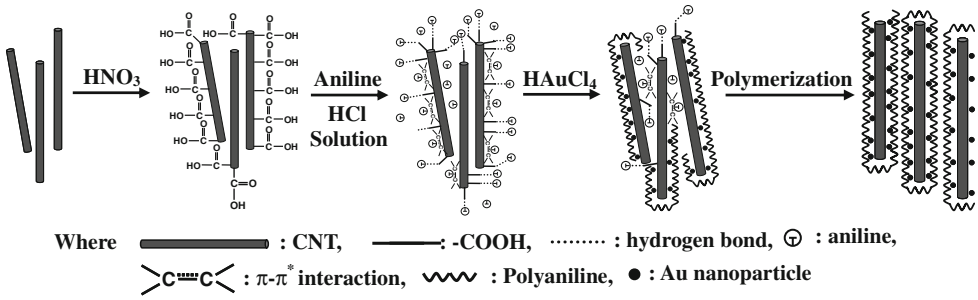

Fig. 1 Schematic drawing of the mechanism governing the formation of Au/PANI/MWNT nanocomposites

and PANI in situ polymerized cause by the strong interaction between MWNTs and aniline monomers. Although there are carboxylic groups on the defect sites of MWNTs to increase the solubility of MWNTs in HCl solution, some MWNT bundles remain randomly configured. Consequently, some gaps may exist between individual MWNTs to allow the aniline monomers to wriggle into such gaps, followed by in situ polymerization cause by the strong interaction between MWNTs and aniline monomers. The growing PANI polymer chain would wedge away the MWNT bundles and then break down the bundles into individual MWNTs. In this case, MWNTs are uniformly and individually dispersed into PANI matrices. The site-selective interaction between the quinoid ring of the polymer and MWNTs caused PANI polymer chains to be adsorbed at the surface of the MWNTs and formed the shell of the tubular nanocomposites [27].

Figure 2 shows typical TEM image of the Au/PANI/MWNT nanocomposites. Clearly, a tubular layer of a highly uniformly coated PANI film is present on the MWNTs surface, and the diameter of the as-prepared tubular Au/PANI/MWNT nanocomposites is about 150–200 nm. And, the diameter of the original MWNTs is 20–40 nm. The image reveals that the resulting Au/PANI/MWNT nanocomposites is the typical core-shell structure, and the MWNTs serves as the core and are individually wrapped by the PANI. The aniline monomers are uniformly polymerized on the MWNTs and form a tubular shell of Au/PANI/MWNT nanocomposites. Besides, the presence of Au nanoparticles can be witnessed from the TEM image. The dark spots in TEM image are the Au nanoparticles. It is to be noted that Au nanoparticles are anchored or decorated on the walls of MWNTs coated with a layer of PANI. It is also likely that a portion of Au nanoparticles may be entrapped in the layer of PANI that could not be noticed on the surface of MWNTs. Because the Au nanoparticles are dispersed in the PANI/MWNT composites and the TEM image is at low magnification, it is hard to estimate the exact particle size of the Au nanoparticles. But the particle size can be determined from the XRD data with Debye–Scherrer formula, which is calculated to be about 20 nm. An electron diffraction (ED) pattern of this area shows the diffraction dots of the gold and the characteristic rings of polymer, which further proves that the nanocomposite consists of amorphous PANI and Au nanoparticles.

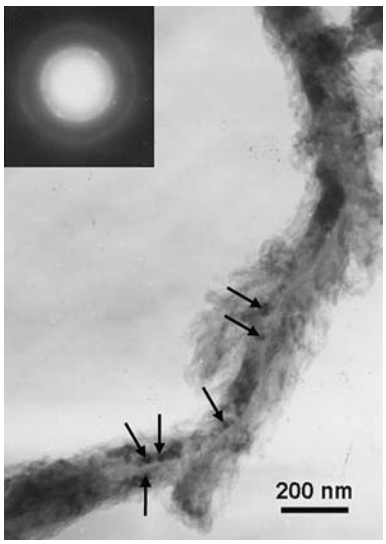

Fig. 2 TEM images of the Au/PANI/MWNT nanocomposites (inset: an ED pattern of the nanocomposites)

FT–IR spectrum (Fig. 3) of PANI and Au/PANI/MWNT nanocomposites is presented. The spectral characteristic of Au/PANI/MWNT nanocomposites mainly resembles PANI. The characteristic bands of PANI at wavenumbers of 1574 cm^{-1} (assigned to the stretching of the quinoid rings), 1492 cm^{-1} (C=C stretching of benzenoid rings), 1296 cm^{-1} (C–N stretching mode), and 1120 cm^{-1} (N=Q=N,Q representing the quinoid ring) are observed clearly in the FT–IR spectrum of the nanocomposites, and are identical to those of the emeraldine salt form of PANI.

XRD pattern recorded from a drop-coated film of the sample on a silica substrate is shown in Fig. 4. The (111), (200), (220), and (311) Bragg reflections of face-centered cubic (fcc) Au are clearly observed [28]. A weak broad peak centered at $2\theta = 26$ may be attributed to the amorphous PANI chain [29]. Results from XRD analysis support the presence of PANI and Au^0 nanoparticles in the nanocomposites.

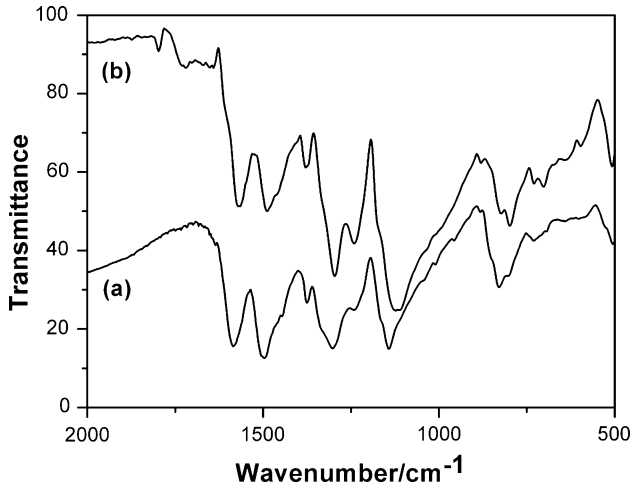

Fig. 3 FT-IR spectrum of (a) PANI and (b) Au/PANI/MWNT nanocomposites

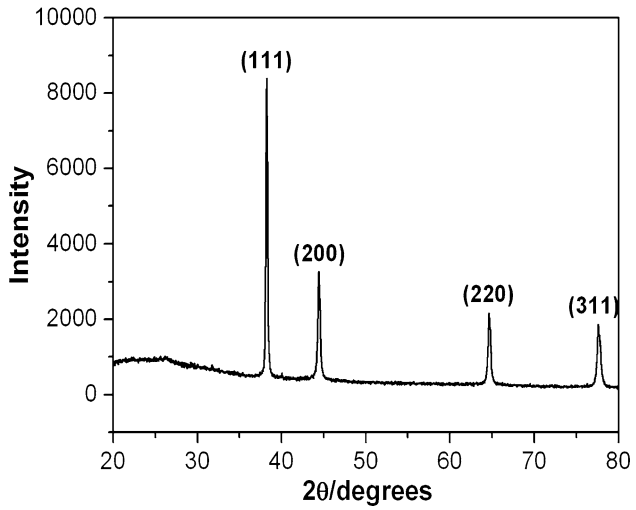

Fig. 4 XRD pattern of the Au/PANI/MWNT nanocomposites

A chemical analysis of the Au/PANI/MWNT nanocomposites is done using XPS. Figure 5 shows the XPS spectrum of the Au 4*f* and N 1*s* of the sample. Figure 5a shows the Au $4f_{7/2}$ and Au $4f_{5/2}$ doublet with the bonding

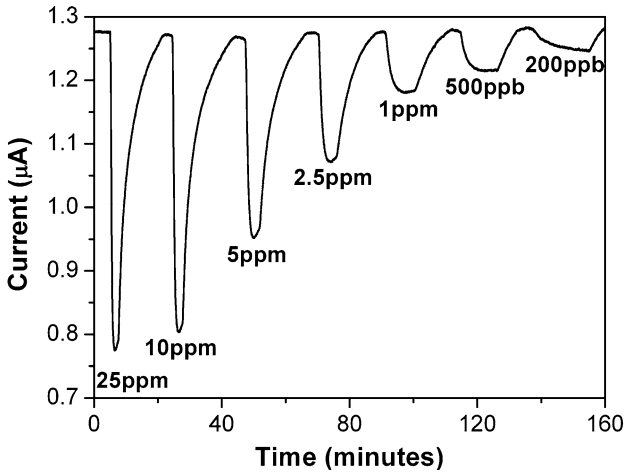

Fig. 6 Real-time detection of the current for different concentration ammonia gas

energies of 83.85 and 87.55 eV, respectively. These are typical value for Au^0 [30]. Figure 5b shows the typical high resolution core-level N 1 *s* spectra of the nanocomposites. The peak appearing at around 399 eV is an indication of the formation of PANI [31].

Figure 6 shows the sensor's response to different concentration of ammonia gas. The resistance of the sensor dramatically increases upon exposed to ammonia gas, and then decreased upon return to pure dry air. Depending on ammonia concentration, the response time of the sensors to ammonia exposure ranged from 1 to 10 min, while the recover time was about 15 min. The sensing mechanism is governed by the protonation/deprotonation phenomena. In the electrically conductive state, PANI is a P-type semiconductor with N^+–H adsorption sites. The resistance change will be modulated by the protonation–deprotonation brought by ammonia gas [32, 33]. As ammonia gas is injected, ammonia gas molecules withdraw protons from N^+–H sites to form energetically more favorable NH_4^+. This deprotonation process reduces PANI from the emeraldine salt state to the emeraldine base state, leading to the reduced hole density in the PANI and thus an increased

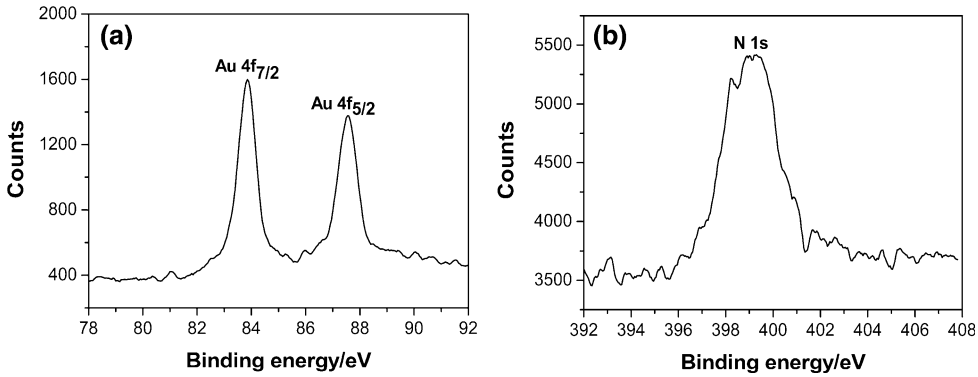

Fig. 5 XPS spectrum of Au 4*f* and N 1 *s* of the Au/PANI/MWNT nanocomposites. (**a**) Au 4*f* and (**b**) N 1 *s*

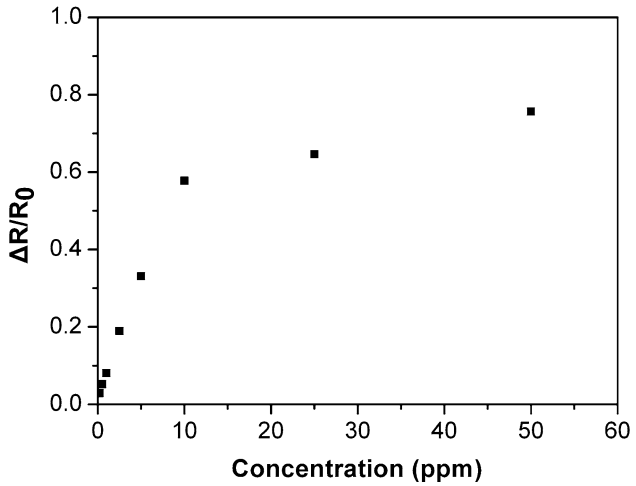

Fig. 7 Sensitivity changes of the Au/PANI/MWNT nanocomposites as a function of ammonia gas concentration

resistance. When the sensor is purged with dry air, the process is reversed, NH_4^+ decomposes to form NH_3 and a proton, and the initial doping level and resistance recover.

Figure 7 shows the sensitivity change of as a function of ammonia gas concentration. The sensitivity is defined as the relative resistance change for a given concentration, or $\Delta R/R_0 = (R_1 - R_0)/R_0$, where R_1 is the steady-state resistance after exposure to ammonia gas and R_0 is the initial resistance before exposure to ammonia gas. It can be seen that the sensors exhibited a linear response of ammonia gas for concentration ranging from 200 ppb to 10 ppm. But when the concentration was above 10 ppm, the sensors displayed a nonlinear response.

A good repeatability or long-term stability is another important parameter of the gas sensor material. Figure 8 represents the electrical response of the Au/PANI/MWNT

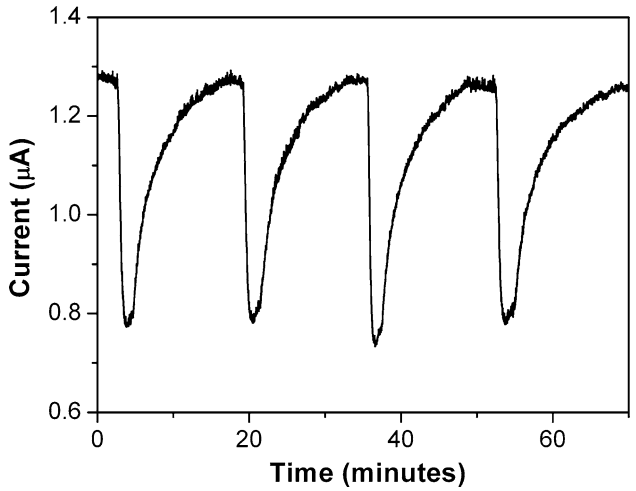

Fig. 8 Repeatability of the Au/PANI/MWNT nanocomposites sensor, the concentration of ammonia gas is 25 ppm

nanocomposites sensor upon periodic exposure to ammonia gas. As the sensor is exposed to ammonia gas, the rapid increment in resistance is observed. After the sensor is purged with dry air, the resistance is observed to recover slowly due to the desorption of ammonia gas molecules from the sensor. The cyclic tests present similar responses more than five times. The mean sensitivity of the sensor response to 25 ppm ammonia gas is 0.638 and the standard deviation is 0.039. Then, we repeat the process a few days later with a number of the Au/PANI/MWNT based sensors and find that the sensors all show a good repeatability. These facts suggest that the sensor have a good repeatability and can be repeatedly used in detecting ammonia gas with excellent stability.

Conclusions

One part synthesis of a nanocomposites comprising of MWNTs, PANI, and Au nanoparticles was successfully established. Carboxylic acid groups contained MWNTs were used as a template for the formation of a composite of doped PANI with MWNTs. Based on the interaction between aniline monomers and c-MWNTs, aniline molecules were adsorbed and then polymerized on surfaces of c-MWNTs. We have also demonstrated a simple method to fabricate Au/PANI/MWNT-based gas sensors. The ammonia gas sensor produced using this method was shown to have superior sensitivity and good repeatability. The novel approach presented herein can be extended to the synthesis of other noble metal based on PANI/MWNT. This is a promising step toward the development of miniaturized devices with extensive analytical capabilities.

Acknowledgements This work was financially supported by the National Natural Science Foundation of China (No. 60574095), the Dean's fund from Hefei Institute of Physical Science, Chinese Academy of Science, and the Knowledge Innovation Program of the Chinese Academy of Science. The authors would like to thank Drs. Tao Luo and Dr. Liangbao Yang for help with preparation of the manuscript.

References

1. Iijima S (1991) Nature 354:56. doi:10.1038/354056a0
2. Dillon AC, Jones KM, Bekkedahl TA, Kiang CH, Bethune DS, Heben MJ (1997) Nature 386:77
3. Chambers A, Park C, Baker RTK, Rodriguez NM (1998) J Phys Chem B 102:4253. doi:10.1021/jp980114l
4. Collins PG, Bradley K, Ishigami M, Zettle A (2000) Science 287:1801. doi:10.1126/science.287.5459.1801
5. Kolmakov A, Moskovits M (2004) Annu Rev Mater Res 34:151. doi:10.1146/annurev.matsci.34.040203.112141
6. Kong J, Franklin NR, Zhou CW, Chapline MG, Peng S, Cho KJ, Dai HJ (2000) Science 287:622

7. Li J, Lu Y, Ye Q, Cinke M, Han J, Meyyappan M (2003) Nano Lett 3:929. doi:10.1021/nl034220x
8. Modi A, Koratkar N, Lass E, Wei B, Ajayan PM (2003) Nature 424:171. doi:10.1038/nature01777
9. Penza M, Cassano G, Aversa P, Antolini F, Cusano A, Cutolo A, Giordano M, Nicolais L (2004) Appl Phys Lett 85:2379
10. Someya T, Small J, Kim P, Nuckolls C, Yardley JT (2003) Nano Lett 3:877. doi:10.1021/nl034061h
11. Cantalini C, Valentini L, Armentano I, Lozzi L, Kenny JM, Santucci S (2003) Sens Actuators B 95:195
12. Zhang J, Boyd A, Tselev A, Paranjape M, Barbara P (2006) Appl Phys Lett 88:123112
13. Bestman K, Lee JO, Wiertz FGM, Heering HA, Dekker C (2003) Nano Lett 3:727
14. Manners I (2001) Science 294:1664
15. Breimer MA, Yevgeny G, Sy S, Sadik OA (2001) Nano Lett 1:305
16. Lu YF, Yang Y, Sellinger A, Lu MC, Huang JM, Fan HY et al (2001) Nature 410:913
17. Boal AK, Ilhan F, DeRouchey JE, Thurnalbrecht T, Russel TP, Rotello VM (2000) Nature 404:746
18. Mu YY, Liang HP, Hu JS, Jiang L, Wan LJ (2005) J Phys Chem B 109:22212
19. Heeger AJ (2001) Angew Chem Int Ed 40:2591
20. Huang JX, Virji S, Weiller BH, Kaner RB (2004) Chem Eur J 10:1314
21. Liu HQ, Kameoka J, Czaplewski DA, Craighead HG (2004) Nano Lett 4:671
22. Wang J, Chan A, Carlson RR, Luo Y, Ge GL, Ries RS, Heath JR, Tseng HR (2004) Nano Lett 4:1693
23. Lee RS, Kim HJ, Fischer JE, Thess A, Smalley RE (1997) Nature 388:255
24. Devi GS, Subrahmanyam VB, Gadkari SC, Gupta SK (2006) Anal Chim Acta 568:41
25. Patil DR, Patil LA, Patil PP (2007) Sens Actuators B 126:368
26. Star A, Stoddart JF, Steuerman D, Diehl M, Bouaki A, Wong EW, Yang X, Chung SW, Chio H, Heath JR (2001) Angew Chem Int Ed 40:1721
27. Cochet M, Maser WK, Benito AM, Callejas MA, Martinez MT, Benoit JM, Schreiber J, Chauevt O (2001) Chem Comm 16:1450
28. Leff DV, Brandt L, Heath JR (1996) Langmuir 12:4723
29. Moon YB, Cao Y, Smith P, Heeger AJ (1989) Polym Comm 30:196
30. Cheng WL, Dong SJ, Wang E (2003) Langmuir 19:9434
31. Dauginet-De Pra L, Demoustier-Champagne S (2005) Thin Solid Flims 479:321
32. Chabukswar VV, Pethkar S, Athawale AA (2001) Sens Actuators B 77:657
33. Kukla AL, Shirshov YM, Piletsky SA (1996) Sens Actuators B 37:135